

Effect of interlayer strain interaction on the island composition and ordering in Ge/Si(001) island superlattices

M. De Seta, G. Capellini,^{a)} and F. Evangelisti

Dipartimento di Fisica, Università di Roma Tre, Via della Vasca Navale 84, 00146 Roma, Italy

C. Ferrari, L. Lazzarini, and G. Salviati

IMEM-CNR Institute, Parco Area delle Scienze 37/A, 43010 Fontanini, Italy

R. W. Peng and S. S. Jiang

National Laboratory of Solid State Microstructures and Department of Physics, Nanjing University, Nanjing 210093, China

(Received 31 May 2007; accepted 3 July 2007; published online 24 August 2007)

In this article we present a quantitative study of the influence of the number and the thickness of the silicon spacer layer on the optical and structural properties of single and multilayers of self-assembled Ge/Si(001) islands. By means of cathodoluminescence spectroscopy, high resolution x-ray diffraction, and transmission electron microscopy, we will show that the island composition and strain status of single-layer samples do not depend on the silicon cap-layer thickness. On the contrary, we found that the strain interaction existing between island layers separated by a silicon spacer layer 33 nm thick (i.e., ~ 3 times the mean island height), enhances the SiGe intermixing during the deposition of subsequent layers bringing to a composition inhomogeneity of the intermixed islands of about 18% along the stack. This inhomogeneity is not present in samples having a thicker spacer layer (60 nm) although the strain interaction between different layers is strong enough to drive the island stacking along the vertical direction. We conclude that the latter spacer layer thickness allows us to obtain a highly ordered three-dimensional superlattice of an island having a homogeneous size and composition along the stack itself. © 2007 American Institute of Physics. [DOI: [10.1063/1.2771066](https://doi.org/10.1063/1.2771066)]

I. INTRODUCTION

Self-assembled Ge/Si nanostructures are a prototypical system for investigating fundamental growth phenomena occurring within the Stanski–Krastanov growth mode.¹ The fabrication of island multilayers, in which self-assembled island layers are alternated to spacer layers of a different material, offers many advantages since, beside the obvious increase of the active material available, it is a viable path to reduce the inhomogeneity of self-assembled islands and to improve their lateral order.^{2,3}

These phenomena are mainly due to the mutual interaction through the spacer layers of islands belonging to different layers owing to the elastic relaxation of the heteroepitaxial strain. The intensity of the strain interaction increases for decreasing spacer layer thickness.⁴ An upper limit of the spacer layer thickness t_{sp} for the observation of vertical stacking in samples similar to the one here studied is $t_{sp} = 100$ nm.⁴ Therefore, in order to increase the order, one should try to thin down t_{sp} as much as possible. However a spacer layer too thin may result in a “wavy” morphology, hindering the possibility to recover a flat surface needed for the subsequent island layer deposition.⁵ Beside this lower bound limit to t_{sp} , a less trivial limitation is due to the effect of the strain interaction on the island size and composition. As a matter of fact it has been suggested that this interaction

enhances the SiGe intermixing during the piling-up of islands belonging to multiple layers.⁶ This induces fluctuations of the island composition and shape along the stack, detrimental for possible applications.

In this article we investigate by means of cathodoluminescence (CL), high resolution x-ray diffraction (XRD), and transmission electron microscopy (TEM), the influence of the number of periods N_L and of the thickness of silicon spacer layer d_{Si} on the optical and structural properties of Ge/Si(001) island multilayers.

By comparing the CL experimental results with a simple calculation of the band energy alignment along the growth direction, we could quantify the island composition variation along the stack as a function of the spacer layer thickness. By combining CL, XRD, and TEM results we found the optimal growth sequence needed to obtain homogeneous and ordered multilayers.

II. EXPERIMENT

The samples studied in this work were grown by depositing single or multilayers of self-assembled Ge islands alternated with silicon layers of variable thickness, by means of the ultrahigh vacuum chemical vapor deposition technique. The Si(001) substrates were cleaned at 1100 °C in H₂ atmosphere. Subsequently, a 500 nm-thick Si buffer layer was grown from high purity silane at a deposition temperature of 800 °C. All the Ge island layers investigated in the present study were deposited at $T=750$ °C using high-purity ger-

^{a)}Author to whom correspondence should be addressed; electronic mail: capellini@fis.uniroma3.it

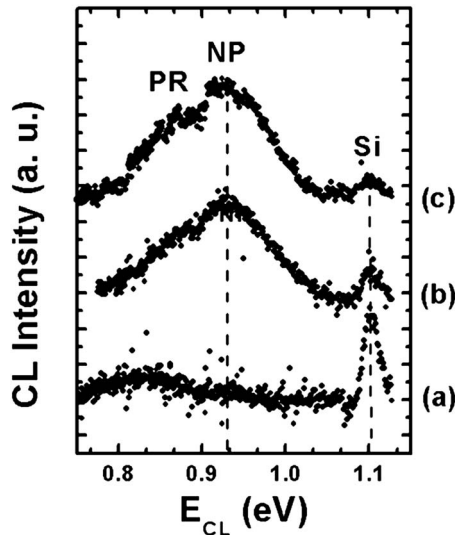


FIG. 1. 77 K CL spectra of samples obtained covering a single Ge island layer with a Si overlayer thickness: (a) $d_{\text{Si}}=10$ nm, (b) $d_{\text{Si}}=18$ nm, and (c) $d_{\text{Si}}=33$ nm.

mane without carrier gas. The germane pressure was 0.4 mTorr with a resulting growth rate of 0.6 \AA/s . The equivalent thickness of the deposited Ge island layers was 1.7 nm. The morphological description of island layers deposited in identical condition may be found in Ref. 7. The silicon cap/spacer layers were deposited at a deposition temperature of $T=750 \text{ }^\circ\text{C}$, using a silane pressure of 0.7 mTorr with a resulting growth rate of 1 \AA/s .

The CL spectroscopy measurements were carried out as a function of sample temperature and injection power conditions by means of a Gatan MonoCL2 system using a LN-cooled North Coast Ge detector attached to a Cambridge 360 Stereoscan scanning electron microscope. The experimental condition used in the CL measurement ($E_b=5 \text{ keV}$, $I_b=540 \text{ nA}$) here reported guaranteed the emission from the complete stacking sequence.

The structural properties of the samples were investigated by a JEOL 2000FX transmission electron microscope operating at 200 keV. The samples were prepared in the (110) cross section geometry by standard mechanochemical procedures followed by ion beam thinning in a Gatan duo mill system.

High resolution x-ray diffraction experiments were performed using an Expert-Pro Philips diffractometer equipped with a four crystal monochromator having a residual divergence of the x-ray beam of 15 arc sec. Reciprocal lattice maps were acquired using the (004) symmetrical and (224) asymmetrical geometries in order to understand the origin of the diffraction peak broadening and to rule-out the presence of plastic strain relaxation through introduction of dislocations.

III. RESULTS AND DISCUSSION

In Fig. 1 we display the CL spectra collected at $T=77 \text{ K}$ of three samples obtained covering a single Ge island layer with a silicon layer of increasing thickness: (a) 10, (b) 18, and (c) 33 nm.

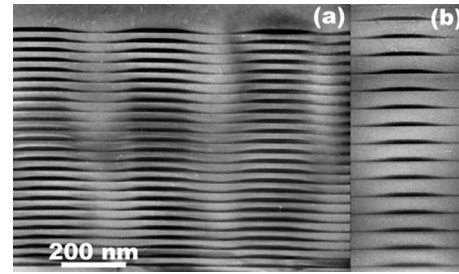


FIG. 2. (110) TEM cross-sectional images taken along the [001] direction of the 33 nm (a) and the 60 nm (b) spacer 25-fold multilayer. Notice that the two images have been displayed using the same magnification.

In spectra (b) and (c) we can observe the silicon phonon-assisted emission centered around $E_{\text{CL}}(\text{Si}) \sim 1.1 \text{ eV}$ and a broad structure made of two emission peaks centered at $E_0=0.938 \text{ eV}$ and $E_1=0.880 \text{ eV}$ that we attribute to the luminescence emission from the buried island layer. The energy splitting of about 60 meV existing between the two peaks is compatible with a no-phonon emission (NP) and a phonon replica (PR), due to the emission of a silicon transverse optical phonon.⁸ In spectra related to samples having a thinner coverage (a), we did not observe any significant contribution from the islands. This is due to the fact that, at this stage of the silicon overgrowth, the supplied silicon atoms are mainly incorporated into the islands,⁷ leaving the surface of the intermixed island exposed to ambient oxidation. This surface degradation enhances the probability of nonradiative recombination of the electron-holes pairs generated by the electronic beam with a consequent quenching of the emitted intensity.

The striking feature of Fig. 1 is the independence of the NP peak position from the cap-layer thickness. As a matter of fact, we could expect an energy shift of the CL emission whenever the island shape, strain status, or composition are modified by the capping process.

In order to study how the strain interaction affects the structural and optical properties of Ge(Si)/Si multilayers we have prepared two samples made of a $N_L=10$ and $N_L=25$ island layers separated by a $d_{\text{Si}}=33 \text{ nm}$ thick silicon layer and a third sample having $N_L=25$ island layers and $d_{\text{Si}}=60 \text{ nm}$.

In Fig. 2(a) we report the cross-sectional TEM images of the 25-fold stack having $d_{\text{Si}}=33 \text{ nm}$ and in panel (b) a detail (the bottom 15 layers) of an island column belonging to the 25-fold, $d_{\text{Si}}=60 \text{ nm}$ multilayer sample.

In both samples, the islands belonging to different layers are well aligned along the (001) direction (henceforth the z direction). This evidences that the spacer layer is thin enough to induce the vertical correlation between islands and large enough to recover a flat surface before the growth of the subsequent layer, in agreement with previous results.^{7,9}

The buried island shape is that of a truncated pyramid with mean base $b \sim 200 \text{ nm}$, mean height $h \sim 10 \text{ nm}$, and aspect ratio $\alpha=h/b \sim 0.05$.

In Fig. 3(a) we present the CL spectra acquired at a temperature $T=77 \text{ K}$ on the samples having $d_{\text{Si}}=33 \text{ nm}$ and different N_L . The shape of the spectral emission is qualitatively similar in all the samples and it is dominated by the

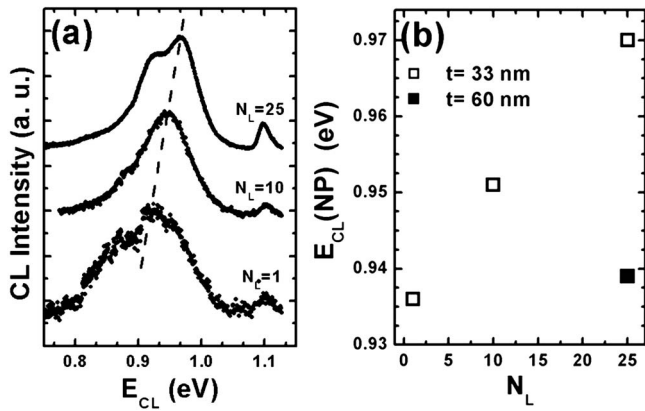


FIG. 3. (a) 77 K CL spectra of a samples with 33nm-thick silicon spacer. (b) No-phonon line energy as a function of the number of layer of 33 nm (open squares) and 60 nm (closed square) thick silicon spacer samples.

NP+PR peaks emission from the islands with a weak contribution at higher energy due to silicon layers. However, the island-related spectral features are progressively blueshifted for increasing N_L . In Fig. 3(b) we report the NP peak energy as a function of N_L for both the $d_{\text{Si}}=33$ nm (open squares) and the $d_{\text{Si}}=60$ nm (closed squares) thick silicon spacer layer samples. The NP energy increases in the thinner spacer layer samples, while it is almost independent of the number of island layers in the thicker spacer layer sample.

The energy of the luminescence emission due to the optical transitions related to the islands is influenced essentially by: (i) the size and shape of the islands; (ii) their actual composition, i.e., the degree of intermixing; and (iii) the energy-band alignment at the interfaces. The band alignment is in turn strongly influenced by the heteroepitaxial strain.

In samples similar to those studied here, we have measured an average island composition of $x \sim 0.3$ by means of x-ray absorption.⁷ For this reason we assume in the following that the band alignment is of type II, according to recent calculations by El Kurdi and co-workers¹⁰ and Virgilio and Grosso.¹¹

With this assumption the recombination occurs from electrons confined in the silicon layers and holes confined in the Ge(Si) islands, i.e., it is a spatially nondirect recombination. Owing to the large island size we can neglect the contribution of the carrier quantum confinement to the transition energy and write the emission energy as

$$E_{\text{CL}} = E_c^{\text{min}} - E_v^{\text{max}}.$$

Given the type II alignment here, E_c^{min} is the silicon conduction band minimum while E_v^{max} is the top of the intermixed GeSi island valence band. These energies depend on the strain, present both in the Si spacer layer and in the GeSi island layer, due to the elastic relaxation of the heteroepitaxial mismatch. The tensile strain in the silicon layers induces an increase of the conduction band offset close to the interface by lowering the Δ_2 -Si conduction band. The compressive strain in the Ge islands pushes the heavy-holes band E_{hh} at higher energy: as a consequence $E_v^{\text{max}} = E_{\text{hh}}$ and has Γ symmetry.

From the previous scheme and following Ref. 12, E_{CL} can be written as

$$E_{\text{CL}} = E_{\text{Gap}}(\text{Si}) - \Delta E_v^{\text{av}} - \Delta E_{\Delta(2)}^{\text{Si}} - \Delta E_{\text{hh}}^{\text{GeSi}},$$

where $E_{\text{Gap}}(\text{Si}) = 1.181$ eV is the Si energy gap at 77 K, ΔE_v^{av} is the discontinuity of the weighted average of the valence bands (independent of the strain), while $\Delta E_{\Delta(2)}^{\text{Si}}$ and $\Delta E_{\text{hh}}^{\text{GeSi}}$ are, respectively, the energy offset of the Si conduction band edge and of the Ge valence band edge resulting from the strain tensor ε_{ij} . The latter two terms can be written as¹² (all the energies are expressed in eV)

$$\Delta E_{\Delta(2)}^{\text{Si}} = 6.11 |(\varepsilon_{zz}^{\text{Si}} - \varepsilon_{yy}^{\text{Si}})|$$

and

$$\Delta E_{\text{hh}}^{\text{GeSi}} = \frac{1}{3} \Delta_0(\text{Ge}_x\text{Si}_{1-x}) + 2.55(\varepsilon_{zz}^{\text{Ge}_x\text{Si}_{1-x}} - \varepsilon_{yy}^{\text{Ge}_x\text{Si}_{1-x}}).$$

If we assume that a linear interpolation holds for $\Delta E_v^{\text{av}} = 0.52x$ and for the experimental spin-orbit splitting at $\Gamma_{25'}$ in the unstrained material $\Delta_0(\text{Ge}_x\text{Si}_{1-x}) = 0.042 + 0.26x$, we can write the emission energy at 77 K as^{8,12}

$$E_{\text{CL}} = 1.167 - 0.52x - \frac{1}{3}(0.26x) - 2.55(\varepsilon_{zz}^{\text{Ge}_x\text{Si}_{1-x}} - \varepsilon_{xx}^{\text{Ge}_x\text{Si}_{1-x}}) - 6.11(\varepsilon_{xx}^{\text{Si}} - \varepsilon_{zz}^{\text{Si}}). \quad (1)$$

This expression quantifies the dependence of the emission energy on the island average composition x and its strain status and we shall use it to quantitatively discuss our experimental results.

We have recently demonstrated in single layer samples grown in identical experimental conditions^{7,9} that a strong intermixing effect is present in the first stage of the Si cap-layer deposition (i.e., $d_{\text{Si}} \leq 10$ nm), while the intermixing process is hindered for further Si deposition: after the completion of few silicon monolayers on the top of intermixed islands, the island shape and composition are practically “frozen” because bulk diffusion plays a minor role at this process temperature.^{7,9} Given that in samples (b) and (c) of Fig. 1 we have a well formed cap layer, the peak energy stability as a function of the cap-layer thickness confirms our previous findings on the island composition and suggests that the strain status at the interface does not change when the cap-layer thickness is increased.

The fact that the same E_{CL} values is observed in multilayer samples with $d_{\text{Si}}=60$ nm suggests that the island composition and strain status is maintained when $N_L=25$ layers are deposited.

On the contrary, the shift of the emission energy observed in the multilayer sample having 33 nm-thick spacer layers implies that the Ge content of the islands and/or the strain relaxation are influenced by the strain interaction existing between different island layers.

To quantify the effect of the presence of underlying island layers on the island composition we have calculated the emission energy E_{CL} at 77 K as a function of the Ge content x of the islands. We have used expression (1) with the strain fields estimated on the basis of the results obtained by Schmidt and co-workers on multilayer of islands having similar shape,⁸ rescaled to the island sizes, and spacer layer thickness here studied.^{4,13} In Fig. 4 we report the emission

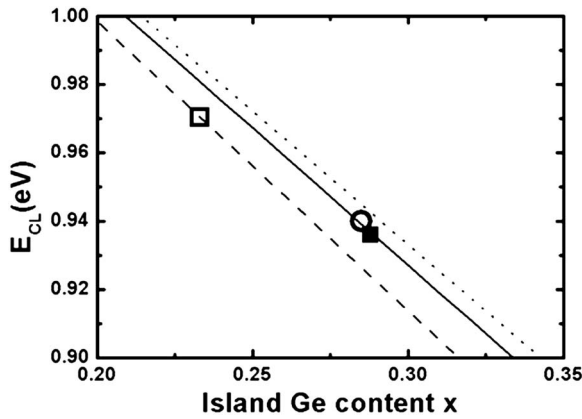


FIG. 4. Emission energy E_{CL} at 77 K as calculated for: (dotted line) an elastically relaxed $\text{Ge}_x\text{Si}_{1-x}$ island embedded in a silicon matrix; (solid line) a single strained island layer enclosed in a relaxed silicon layer; and (dashed line) an island multilayer with a 33 nm-thick spacer layer. The measured E_{CL} are also reported for: (open square) 25-fold multilayer $d_{\text{Si}}=33$ nm, (open circle) 25-fold multilayer $d_{\text{Si}}=60$ nm, and (square) single island layer capped by a $d_{\text{Si}}=33$ nm thick silicon overlayer.

energy E_{CL} at 77 K as calculated for: (dotted line) an elastically relaxed $\text{Ge}_x\text{Si}_{1-x}$ island embedded in a silicon matrix; (solid line) a single strained island layer enclosed in a relaxed silicon layer; and (dashed line) an island multilayers with a 33 nm-thick spacer layer. The calculated E_{CL} in the case of the 60-nm-spaced stack is practically coincident, in the x range here considered, with the single layer case. This is in agreement with the constant measured value of E_{CL} for an increasing number of layer in 60 nm-spaced samples [see Fig. 3(b)].

As can be seen, the effect of the strain interaction between different island layers at a given island composition x , is to decrease the emission energy E_{CL} . The observed experimental increase of E_{CL} for an increasing number of layer N_L in the 33 nm-spacer layer series (see Fig. 4), implies therefore that the interlayer strain correlation has also an indirect effect on E_{CL} through the enhancement of the island alloying.

By equalizing the measured emission energies and the calculated $E_{CL}(x)$ values, the average Ge content in the island layer x can be extracted (see Fig. 4).

The average Ge concentration in the islands as determined by CL in the “thin”-spacer series decreases from $x=0.28$ for $N_L=1$ to $x=0.23$ for $N_L=25$. The agreement of the Ge content values with the one determined on the same sample by means of the x-ray absorption spectroscopy⁷ in the $N_L=1$ case (Fig. 4, square), confirms the validity of band parameter and strain model we have used and allows us to extract quantitative information from the CL analysis. Therefore, the observed blueshift as a function of the number of layers in thin-spacer samples indicates that the strain interaction existing between island layers enhances SiGe intermixing resulting in a Ge content variation along the island stack of the order of 18%.

This Ge content variation is explained in the following way: the silicon lattice in each Si cap layer is highly tensile deformed⁴ due to the presence of the underlying elastically relaxed Ge islands. This effect promotes the diffusion of Ge

and Si atoms during the deposition of each Si spacer layer and their intermixing.¹⁴ As a matter of fact, the Ge-Si interdiffusion helps to relieve the strain energy by reducing the heteroepitaxial lattice mismatch. After the first deposited island layer, the island belonging to subsequent layers will nucleate in register with the underlying ones.⁴ For thin enough spacer layers, the tensile deformation adds-up in subsequent Si spacer layers.⁸ The increased tensile deformation in the Si spacer layer enhances the SiGe alloying during the deposition of the multilayered structure leading to more intermixed islands as N_L increases. With the typical shape and size of our islands (defined by h , b , and α) this strain accumulation is finite and saturates for $N_L \sim 5-10$ island layers⁸ in sample having $d_{\text{Si}}=33$ nm, while it is negligible in samples having a $d_{\text{Si}}=60$ nm. Thus in the case of the thinner spacer samples we can envisage a variation of the island composition in the first layers of the stack. Only when the strain increase in the Si spacer layers is faded out, the subsequent deposited island layers have a constant concentration. Within this framework, we can predict a blueshift of the CL emission peaks with increasing N_L . The blueshift ends when the contribution to the whole signal from the first not homogeneous layers becomes negligible. A peak broadening is expected for small N_L followed by a peak narrowing for larger N_L , as we have observed in the CL spectra of our $d_{\text{Si}}=33$ nm multilayers.

In contrast, the absence of strain accumulation in subsequent layers drives no major effect on the 60 nm-spaced series, although the strain interaction between different layers is strong enough to align vertically the islands as evident in Fig. 2. In this case the islands belonging to different layers have the same composition.

A more statistically significant understanding of the island ordering and homogeneity in these multilayers can be obtained from XRD measurements.

In Fig. 5 we report the (004) symmetrical (angle of incidence equivalent to the angle of emergence) x-ray reciprocal lattice maps represented in the ω , $\omega-2\theta$ space of the samples having $N_L=25$, and spacer layer thickness $d_{\text{Si}}=33$ nm (a) and $d_{\text{Si}}=60$ nm (b), respectively. In both maps the regular spacing of the superstructure peaks along the scattering vector allows the determination of the superlattice period and the average Ge content with a good accuracy using the well known formula $T=\lambda/2\Delta\vartheta \cos \vartheta_B$ in which λ , $\Delta\vartheta$, ϑ_B are the x-ray wavelength, the superlattice period, and the Bragg angle, respectively. In Table I we report the results of the fitting of experimental x-ray diffraction profiles by means of a code based on the dynamical theory of x-ray diffraction.

Within the framework of the effective medium approximation (EMA), each of the $\text{Ge}(\text{Si})$ island layers was replaced in the simulation by a continuous $\text{Ge}_y\text{Si}_{1-y}$ layer having thickness $d(\text{Isl})_{\text{XRD}}=14$ nm, i.e., the mean island height measured from the bottom of its wetting layer, as measured by TEM. The average composition $y=\langle x \rangle_{\text{EMA}}$ and the multilayer periodicity were left as fitting parameters.

From the concentration $\langle x \rangle_{\text{EMA}}$ and the knowledge of the island density and average volume as obtained by TEM and atomic force microscopy measurements⁷ a simple calculation

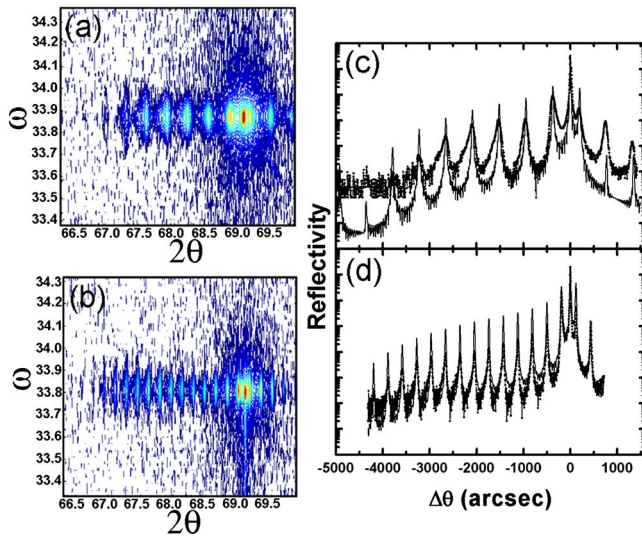


FIG. 5. (Color online) High resolution XRD reciprocal lattice map near the (004) $\text{Cu}(K_{\alpha})$ diffraction of $N_L=25$ structures with 33 (a) and 60 nm (b) thick Si spacer layer in the ω , $\omega-2\theta$ space (degrees). In (c) and (d) we display the experimental (dot) and simulated (solid lines) profiles of the high resolution x-ray rocking curve as obtained by sectioning the reciprocal space map in (a) and (b) along the $\omega-2\theta$ axis.

gives the average island layer composition x_{XRD} . The resulting values are in good agreement with those derived from the CL measurements for both the samples. The XRD line-shape can be used to quantify the concentration fluctuation along vertical direction of the EMA multilayer. To this purpose we display in Figs. 5(c) and 5(d) the comparison between experimental and simulated profile for the $d_{\text{Si}}=33$ nm and $d_{\text{Si}}=60$ nm multilayers, respectively. The XRD data exhibit a broadening of the superlattice peaks in the $\omega-2\theta$ direction, normal to the diffracting planes, of $\delta\theta_0=55$ arc sec. This uniform broadening of the superlattice peaks, independent of the peak order, is interpreted through simulation of the diffraction profile as a variation of the average Ge island layer content along the stack,¹⁵ the superlattice (SL) periodicity remaining constant. This variation of the Ge content can be evaluated in this way: the zeroth order peak of the SL reflectivity curve, corresponding to the Bragg peak of an equivalent GeSi layer with the same average Ge content, is at $\Delta\theta_0=-376$ arc sec with respect to the Si(004) diffraction peak. The observed peak broadening is then induced by a change $\delta\langle x \rangle$ in the average $\langle x \rangle$ Ge content given by

$$\delta\langle x \rangle = \frac{\delta\theta_0}{\Delta\theta_0} = \frac{55 \text{ arc sec}}{376 \text{ arc sec}} = 14.6\%.$$

Thus, in agreement with what obtained by means of the CL data analysis, the XRD analysis evidences a $\sim 15\%$ Ge con-

TABLE I. Thickness and composition as obtained from of the XRD profile fitting procedure on the nominal 33 and 60 nm-thick Si spacer samples assuming uniform SiGe layers.

d_{nom} (nm)	d_{XRD} (nm)	$d_{\text{XRD}}(\text{Si})$ (nm)	$\langle x \rangle_{\text{EMA}}$	x_{XRD}
33	33.9	19.9	0.086	0.23
60	62.2	48.2	0.093	0.25

centration fluctuation along the island stack in the $d_{\text{Si}}=33$ nm sample.

On the contrary the much narrower SL peaks of sample B in the $\omega-2\theta$ direction confirms the good composition stability of the GeSi islands in the sample having $d_{\text{Si}}=60$ nm. In this sample all the SL peaks exhibit peak widths comparable to that expected for a uniform composition superlattice.

Both reciprocal lattice maps of the 33 and 60 nm-thick sample show superlattice peaks broadened in a direction perpendicular to the (004) scattering vector. The diffuse scattering perpendicular to the scattering vector arises from the in plane strain modulation induced by the GeSi islands.¹⁶ In our experimental conditions, it is difficult to identify unambiguously a signature of the in plane island ordering into the reciprocal lattice map, owing to the large island-island in-plane distance of 300 nm, i.e., 5–10 times larger than the vertical period d_{Si} (see Fig. 2). However, we have found in similar samples that the buried islands are arranged on a square lattice in the growth plane,^{17,18} evidencing the achievement of a three-dimensional island ordering in these multilayers.

IV. CONCLUSIONS

In summary we have investigated the optical and structural properties of UHV-CVD-grown Ge(Si)/Si(001) island multilayers and determined the island composition and the composition homogeneity as a function of the spacer layer thickness and the number of island layers. To this purpose we have used a model that takes into account the effect of the strain and composition on the CL emission energy.

In samples made of a single island layer, the emission energy is independent of the Si overlayer thickness and we found an island average Ge content $x \sim 0.3$. On the contrary, the blueshift of the emission energy observed in multilayers with $d_{\text{Si}}=33$ nm evidences a variation of the island composition along the island stack of the order of 15%–18% with respect to the average composition $x=0.23$. This composition variation has been interpreted as due to the strain accumulation along the stack that saturates after 5–10 island layers. This detrimental effect, confirmed by the XRD analysis, is not observed in multilayers with $d_{\text{Si}}=60$ nm, although the island-island interaction is sufficient to pile-up the islands. We therefore conclude that in order to obtain a well ordered island superlattice made of islands of constant composition and shape it is necessary to choose a spacer layer thickness in the range 50–70 nm, i.e., of the order of 5–7 times the island height.

¹K. Brunner, Rep. Prog. Phys. **65**, 27 (2002).

²V. A. Shchukin and D. Bimberg, Rev. Mod. Phys. **71**, 1125 (1999).

³J. Stangl, V. Holý, and G. Bauer, Rev. Mod. Phys. **76**, 725 (2004).

⁴R. Marchetti, F. Montalenti, L. Miglio G. Capellini, M. De Seta, and F. Evangelisti, Appl. Phys. Lett. **87**, 261919 (2005).

⁵P. Sutter, E. Mateeva-Sutter, and L. Vescan, Appl. Phys. Lett. **78**, 1736 (2001).

⁶O. G. Schmidt and K. Eberl, Phys. Rev. B **61**, 13721 (2000).

⁷G. Capellini, M. De Seta, L. Di Gaspare, F. Evangelisti, and F. d'Acapito, J. Appl. Phys. **98**, 124901 (2005).

⁸O. G. Schmidt, K. Eberl, and Y. Rau, Phys. Rev. B **62**, 16715 (2000).

⁹M. De Seta, G. Capellini, L. Di Gaspare, F. Evangelisti, and F. d'Acapito, J. Appl. Phys. **100**, 093516 (2006).

- ¹⁰M. El Kurdi, S. Sauvage, G. Fishman, and P. Boucaud, *Phys. Rev. B* **73**, 195327 (2006).
- ¹¹M. Virgilio and G. Grosso, *J. Phys.: Condens. Matter* **18**, 1021 (2006).
- ¹²C. G. Van de Walle and R. M. Martin, *Phys. Rev. B* **34**, 5621 (1986).
- ¹³F. Montalenti, A. Marzegalli, G. Capellini, M. De Seta, and L. Miglio, *J. Phys.: Condens. Matter* **19**, 225001 (2007).
- ¹⁴L. Huang, F. Liu, G.-H. Lu, and X. G. Gong, *Phys. Rev. Lett.* **96**, 016103 (2006).
- ¹⁵P. Fewster, *Semicond. Sci. Technol.* **8**, 1915 (1993).
- ¹⁶U. Pietsch, V. Holý, and T. Baumbach, *High-Resolution X-Ray Scattering. From Thin Films to Lateral Nanostructures*, 2nd ed. (Springer, Berlin, 2004), p. 371.
- ¹⁷G. Capellini, M. De Seta, F. Evangelisti, and C. Spinella, *Appl. Phys. Lett.* **82**, 1772 (2003).
- ¹⁸G. Capellini, M. De Seta, F. Evangelisti, V. A. Zinovyev, G. Vastola, F. Montalenti, and L. Miglio, *Phys. Rev. Lett.* **96**, 106102 (2006).